

Research Note

## Numerical Simulation of Buoyancy Affected Turbulent Air Flow in a Room

A. Nouri-Borujerdi\* and A. Fathi-Gishnegani<sup>1</sup>

In this paper, a three-dimensional steady state incompressible turbulent air flow is considered in a large single room. The buoyancy affected turbulent air flow is numerically simulated by solving governing equations. The turbulence modeling includes both  $k - \varepsilon$  and zero-equation models and their results are compared to the experimental data. The paper reviews several aspects, such as displacement of radiator system performance, temperature and flow field distribution and comfort conditions. The results show that the best temperature distribution and comfort condition are obtained when the radiator is installed under the window and its height is equal to or greater than that of the window.

### INTRODUCTION

In modern building, it is important to resolve the relationship between geometric room parameters and air flow patterns produced by heating or cooling systems. These parameters have major impacts on the air flow patterns and performance of the heating or cooling systems in the room. The flow that forms in this case is usually incompressible and often turbulent, due to the velocity levels and dimensions involved.

Two approaches of computational simulations are available for the study of indoor air temperature distribution. The first approach is the Computational Fluid Dynamics (CFD) method and the second is a simplified flow simulation method, such as the zonal model. The zonal model approach, which was developed during the last two decades, gives fast approximation, but it is unable to provide the required detailed information.

The CFD method numerically solves a set of partial differential equations for the conservation of mass, momentum and energy equations. The solution provides the field distributions of air temperature and velocity. Because the turbulence models are approximated models, they need to be validated by experimental data before being used as a design tool. Some researchers have made efforts to measure airflow in real rooms or have used small-scale models to

represent a full scale room [1]. However, the experimental methods are much more expensive than CFD techniques and lack the flexibility to simulate various boundary conditions, such as a complex diffuser. With CFD techniques, a whole field distribution can be obtained from the solution, while, in most experiments, the measurements can only be carried out at a few locations in the room.

Ball and Bergman [2] used the Chebyshev collection technique to calculate the enclosure with differentially heated side walls. They calculated the enclosure with different aspect ratios and a range of Rayleigh numbers up to  $10^6$ .

Peeters et al. [3] presented a numerical simulation of a natural convection in a square cavity. A low Reynolds number model was used to study air flow with Rayleigh numbers up to  $10^{14}$ . They found that the position of the laminar to turbulence transition in a vertical boundary layer highly depends on the turbulence model used and that the same Rayleigh number and grid spacing could produce multiple solutions.

Cheesewright et al. [4] measured natural convection in a cavity with a Rayleigh number of  $5 \times 10^{10}$ . Air velocity, temperature and turbulence quantities were measured. They presented a method to correct the influence of the heat lost due to imperfect insulation. The nonsymmetrical boundary layer on hot and cold walls and the relaminarisation at the bottom of a hot wall boundary were found. This experiment was numerically simulated by Chen et al. [5].

Olsen et al. [1] measured natural convection in a full scale room as well as in a small scale model with differentially heated walls. The aspect ratio of the room

\*. Corresponding Author, Department of Mechanical Engineering, Sharif University of Technology, Tehran, I.R. Iran. E-mail: anouri@sharif.edu

1. Department of Mechanical Engineering, Sharif University of Technology, Tehran, I.R. Iran.

was  $H/L = 0.3$ . This is a case very close to a real room. They found turbulent boundary layers on vertical walls and recirculation flows at core regions. This feature was not found in the previous studies on natural convection in an enclosure. This is a very challenging problem that should be studied.

Schwenke [6] conducted a series of experiments on a ventilated room with a heated wall. He investigated the effect of the Archimedes number on mixed convection in a ventilated room. Blay et al. [7] also investigated a ventilated room with heated flow. They measured mean velocity and temperature in a model room. They found that the direction of the eddy at the room center depends on the Froude number of the cavity.

The aim of this study is the prediction of the velocity and temperature distribution for a buoyancy affected turbulent air flow caused by one radiator at different locations in a room. The experimental data was used to verify the accuracy of the numerical results.

## GOVERNING EQUATIONS

Often airflow calculations use the Boussinesq approximation. The approximation takes constant air density in the momentum equation, except in the buoyancy term. The indoor airflows are usually turbulent. With an eddy-viscosity model, the indoor airflows can be described by the following time-averaged Navier-Stokes equations for the steady state conservation of mass, momentum and energy:

$$\frac{\partial}{\partial x_i}(\rho V_i) = 0, \quad (1)$$

$$\frac{\partial \rho V_i V_j}{\partial x_j} = -\frac{\partial P}{\partial x_j} + \frac{\partial}{\partial x_i} \left[ (\mu + \mu_t) \frac{\partial V_i}{\partial x_i} \right] + \rho g_i \beta (T - T_{ref}), \quad (2)$$

$$\frac{\partial \rho C_p V_j T}{\partial x_j} = \frac{\partial}{\partial x_j} \left[ (k + k_t) \frac{\partial T}{\partial x_j} \right] + S, \quad (3)$$

where  $\mu_t$  is eddy viscosity and is defined as follows:

If  $y^+ \leq 30$

The eddy viscosity, based on the Prandtl mixing length hypothesis [8] and the Van Driest [9] damping function to include wall damping effects for the zero equation model is:

$$\mu_t = \rho k^2 y^2 \left[ 1 - \exp\left(-\frac{y^+}{A}\right) \right]^2 \left| \frac{\partial u}{\partial y} \right|, \quad (4)$$

where  $k = 0.41$ ,  $A = 26$  and  $y^+ = y(\tau/\rho)^{0.5}/\nu$ .

If  $y^+ > 30$

Based on the Prandtl-Kolmogorov assumption, the eddy viscosity is expressed as:

$$\mu_t = C_v \rho I k^{0.5} l, \quad (5)$$

where  $C_v = 0.5478$  and  $K$  is turbulent kinetic energy.  $I$  is turbulence intensity and can be expressed through the mean flow velocity as follows:

$$I = \frac{\sqrt{v_i'^2}}{|V|} = \frac{\sqrt{2k}}{\sqrt{u^2 + v^2}}, \quad (6)$$

$$k = \frac{\sqrt{u'^2 + v'^2}}{2}. \quad (7)$$

The average turbulence intensity for indoor air flow is assumed to be 10%. This value is a good estimate for the occupied zone in mixing ventilation, yet it can be far from reality, near or within the jet region.

Chen and Xu [10] used the assumption of uniform turbulence intensity and derived an algebraic equation to express the eddy viscosity as a function of local mean velocity,  $V$ , and a length scale,  $l$ , a distance to the nearest surface of enclosure.

$$\mu_t = 0.03874 \rho l. \quad (8)$$

## CALCULATION PROCEDURE

The room being considered is divided into small control volumes or cells (Figure 1). The differential equations are integrated over each control volume to obtain discretization equations of a finite volume form. The standard QUICK differencing scheme is used to determine the expression of the neighbor coefficient [11] as

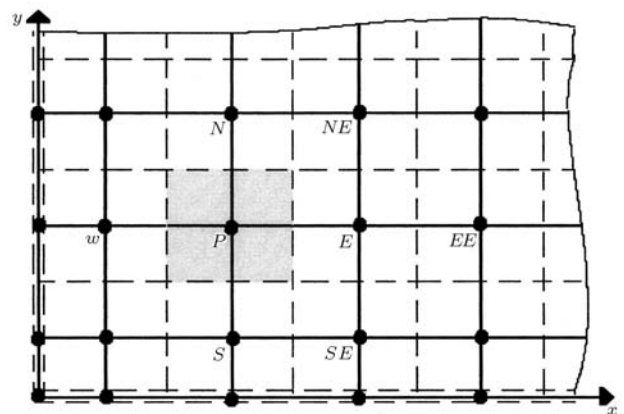


Figure 1. Control volumes and grids for the collocated method.

follows:

$$\begin{aligned} a_P \phi_P &= a_W \phi_W + a_{WW} \phi_{WW} + a_E \phi_E + a_{EE} \phi_{EE} \\ &+ a_N \phi_N + a_{NN} \phi_{NN} + a_S \phi_S + a_{SS} \phi_{SS} \\ &+ a_T \phi_T + a_{TT} \phi_{TT} + a_B \phi_B + a_{BB} \phi_{BB} + b, \end{aligned} \quad (9)$$

where:

$$\begin{aligned} a_W &= D_w + \frac{6}{8} \alpha_w F_w + \frac{1}{8} \alpha_e F_e + \frac{3}{8} (1 - \alpha_w) F_w, \\ a_{WW} &= -\frac{1}{8} \alpha_w F_w, \\ a_E &= D_e - \frac{3}{8} \alpha_e F_e - \frac{6}{8} (1 - \alpha_e) F_e - \frac{1}{8} (1 - \alpha_w) F_w, \\ a_{EE} &= \frac{1}{8} (1 - \alpha_e) F_e, \end{aligned}$$

with:

$$\begin{aligned} \alpha_w &= 1, \text{ for } F_w > 0, & \text{ and } & \alpha_e = 1, \text{ for } F_e > 0, \\ \alpha_w &= 0, \text{ for } F_w < 0, & \text{ and } & \alpha_e = 0, \text{ for } F_e < 0. \end{aligned}$$

Other neighbor coefficients are calculated the same as  $a_W$ ,  $a_E$ :

$$b = S_C \Delta x \Delta y \Delta z,$$

$$a_P = a_W + a_E + a_S + a_N + a_B + a_T - S_P \Delta x \Delta y \Delta z, \quad (10)$$

where  $a_i$ s are the neighbor coefficients representing the convection and diffusion flux at the cell boundary surfaces. The subscripts  $W$ ,  $E$ ,  $S$ ,  $N$ ,  $B$  and  $T$  represent the neighbor grids of  $P$  as shown in Figure 1;  $S_c$  and  $S_p$  are the linearization coefficients of the source term,  $S$ , in Equation 3 [12].

The QUICK differencing scheme is used to determine the expression of the neighbor coefficient [11]. The SIMPLE algorithm is used with the collocated grid for solution of the finite difference governing partial differential equations to the control volume approach.

The boundary conditions required for governing equations are as follows:

a) On the adiabatic walls:

$$\begin{bmatrix} u \\ v \\ w \end{bmatrix} = \begin{bmatrix} 0 \\ 0 \\ 0 \end{bmatrix}, \quad \frac{\partial T}{\partial n} = 0, \quad (11)$$

where  $n$  is a local normal direction to the wall.

b) On the radiator and window:

$$T_{\text{rad}} = T_h, \quad T_{\text{win}} = T_c. \quad (12)$$

## RESULTS AND DISCUSSION

A CFD program with a zero equation turbulence model has been developed. The program provides a source code that can be easily changed to study the model performance and numerical algorithm. In this section, the first phase focuses on the solution of air velocity and temperature, based on the following circumstances.

### Natural Convection with Differentially Heated Walls

The physical model selected for this case is a two dimensional rectangular enclosure with a height of 2.5 m and a length of 7.9 m.

The experimental work of Olsen indicates a recirculation flow on the ceiling and floor with two large eddies at the upper-right and the lower-left corners. Olsen argued that this is because the horizontal mass flow rate on the ceiling is too great to entrain entirely into the cold wall boundary layer. After turning down, the outer portion of the flow goes upward, forms the eddy and reverses the flow. This suggests that a buoyancy force in the corner region is important.

Figure 2 shows the distribution of the room air temperature along the  $x$ -axis on the floor. The abscissa and ordinate of the figure are dimensionalized by the room length ( $L = 7.9$  m) and the difference between the hot and cold wall temperatures ( $T_h - T_c$ ), respectively. It is found that, at a distance of about  $x/L = 0.01$  from the wall, the room air temperature approaches a constant value. The results of the present work also show that there is a good agreement between the numerical solution and the experimental data of Olsen et al. [1].

A similar plot, but in the vertical direction of the room, is depicted in Figure 3. In comparison with Olsen's data, a good agreement is found at the core,

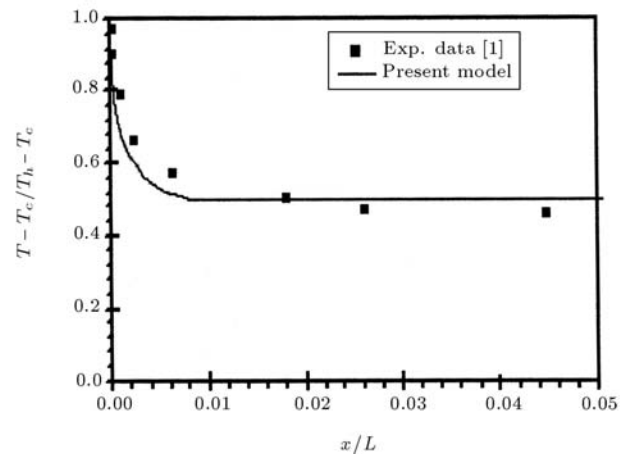
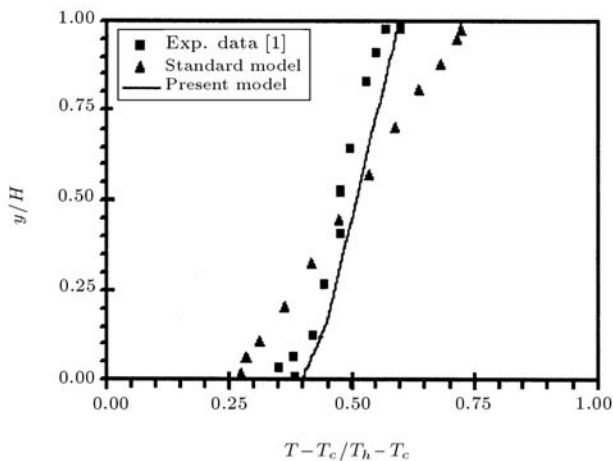


Figure 2. Room air temperature distribution along the  $x$ -axis (horizontal direction).



**Figure 3.** Room air temperature distribution along the  $y$ -axis (vertical direction).

but not near the wall regions. This may be because of the imperfect insulation in the experimental work, which caused heat loss and/or gain to the ceiling or from the floor.

### Natural Convection in a Room Including One Window and One Radiator

In this section, the combined fluid flow and heat transfer is simulated in a three dimensional room for various radiator dimensions and displacement.

Figure 4 illustrates a room including one window and one radiator as a heat sink and a heat source, respectively. The room dimensions are 5 m long, 4 m wide and 3 m high (used by Olsen et al. [1]). The two opposite vertical walls are at  $35.3^{\circ}\text{C}$  and  $19.9^{\circ}\text{C}$ . The ceiling and floor are assumed to be insulated.

The dimensions of the window are 2.5 m wide and 1 m high with a constant temperature ( $T_{\text{win}} = 17^{\circ}\text{C}$ ). The dimensions of the radiator are 1 m wide and 1 m

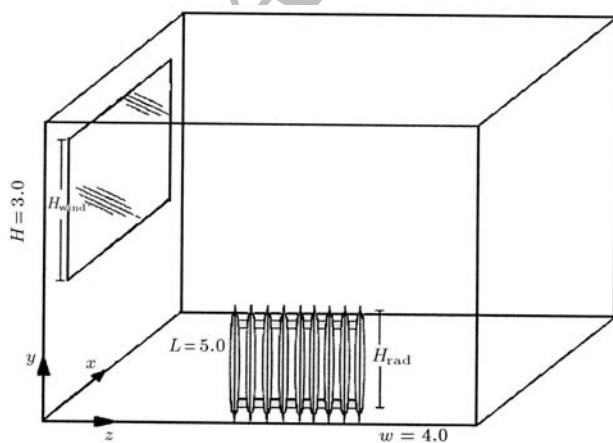


**Figure 4.** Schematic of a room including one window and one radiator.

high with a constant temperature ( $T_{\text{rad}} = 67^{\circ}\text{C}$ ). The Rayleigh number, which is just in the transition regime ( $\text{Ra} = 1.8 \times 10^9$ ), is calculated based on the average height of the window and radiator and the difference between their temperatures.

Figures 5 and 6 illustrate the air flow pattern and temperature contours in the  $z - y$  plane at the middle section of the  $x$ -axis. Figure 7 shows that the temperature contours change across the room from  $T_{\text{rad}}$  next to the radiator to  $T_{\text{win}}$  near the window.

In the second case, the window and radiator are assumed to be installed on two neighboring walls (Figures 7 and 8). These figures are plotted on  $y - z$  and  $y - x$  planes at  $x/L = 0.5$  and  $z/W = 0.5$ , respectively. There is a strong upward warm jet near the radiator and one downward cold jet near the window. Therefore, the cold air penetrates into the middle of the room.

Figures 9 and 10 illustrate the temperature contours on the  $y - z$  and  $y - x$  planes at  $x/L = 0.5$  and  $z/W = 0.5$ , respectively. The results show a non-uniform temperature distribution across the room and some cold regions on the floor of the room.

In the third case, the radiator and the window are

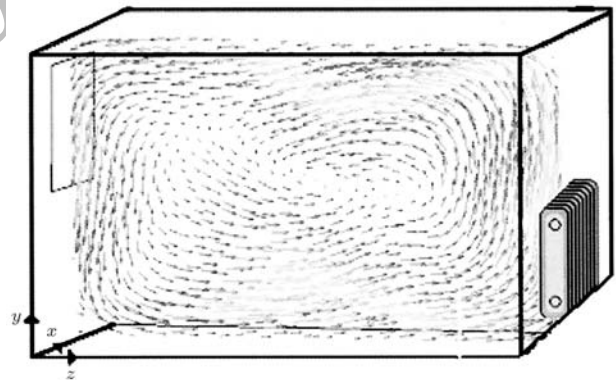


**Figure 5.** Room air flow pattern with one window and one radiator on two opposite walls at  $x/L = 0.5$ .

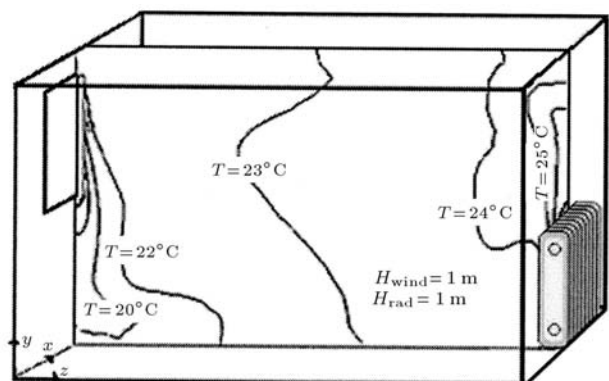


**Figure 6.** Room air temperature contours with one window and one radiator on two opposite wall at  $x/L = 0.5$ .

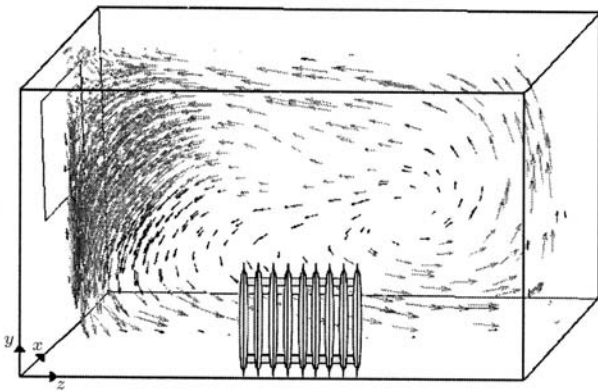


**Figure 7.** Room air flow pattern with one window and one frontal radiator on two neighboring walls at  $x/L = 0.5$ .

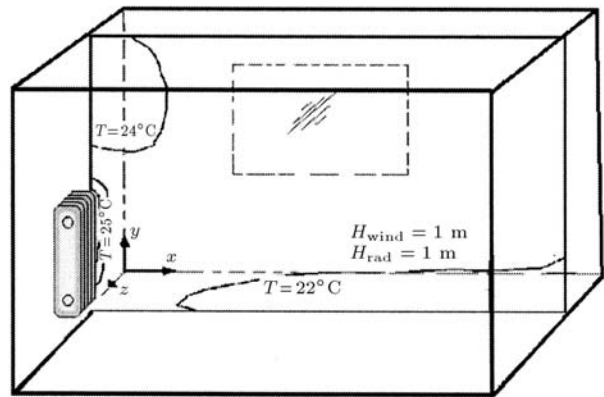


**Figure 10.** Room air temperature contours with one window and one left radiator on two neighboring walls at  $z/W = 0.5$ .

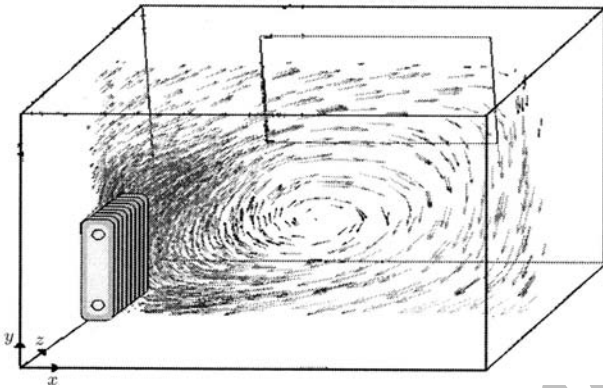


**Figure 8.** Room air flow pattern with one window and one left radiator on two neighboring walls at  $z/W = 0.5$ .

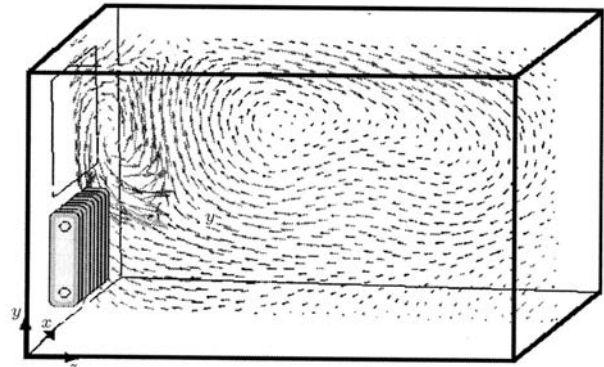


**Figure 11.** Room air flow pattern with one window and one left radiator on the same wall at  $x/L = 0.5$ .

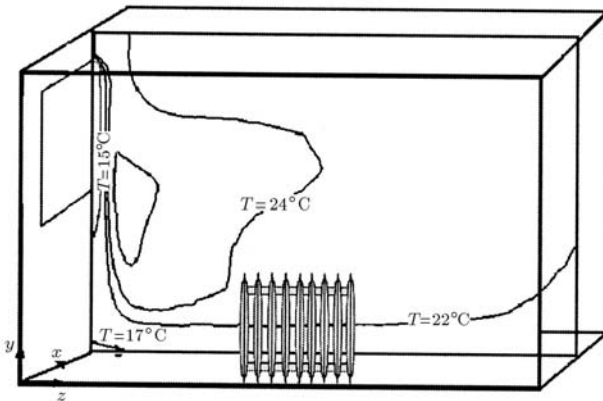


**Figure 9.** Room air temperature contours with one window and one frontal radiator on two neighboring walls at  $x/L = 0.5$ .

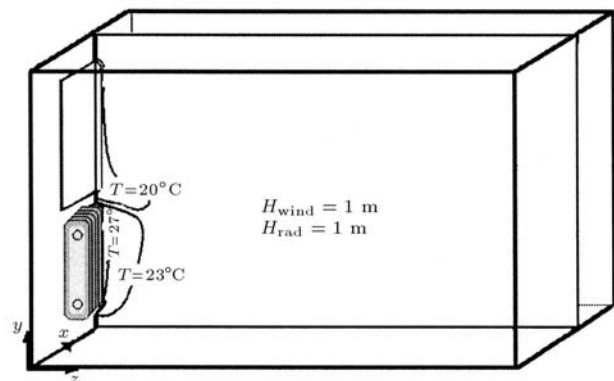


**Figure 12.** Room air temperature contours with one window and one left radiator on the same wall at  $x/L = 0.5$ .

assumed to be installed on the same wall. Figures 11 and 12 are both plotted on the  $y-z$  plane at  $x/L = 0.5$ . There is a strong upward warm jet near the radiator and one downward cold jet near the window. Hence, the cold and hot jets are mixed together and the cold air does not penetrate to the core region of the room.

Thus, a uniform air temperature occupies the rest of the room (Figure 12). This case suggests that the installation of a window and a radiator on the same wall is the best choice for winter heating.

Figures 13 and 14 illustrate two cases in which the radiator heights are different from the same window

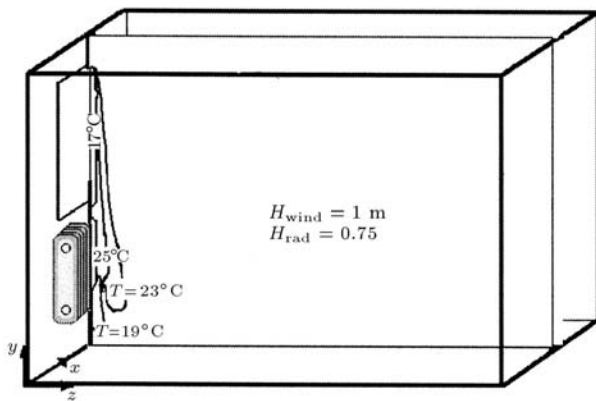


**Figure 13.** Room air temperature contours with one window and one radiator on the same wall at  $x/L = 0.5$ .

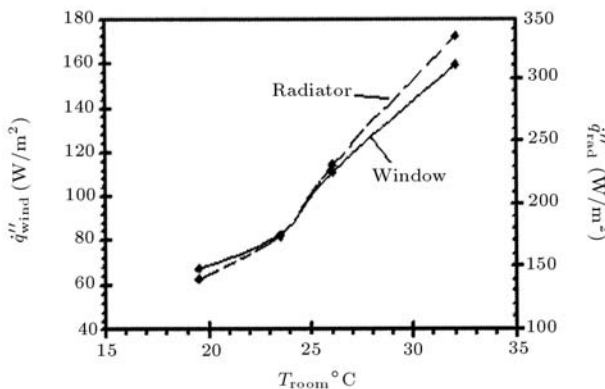


**Figure 14.** Heat flux from the window and radiator vs. room temperature.

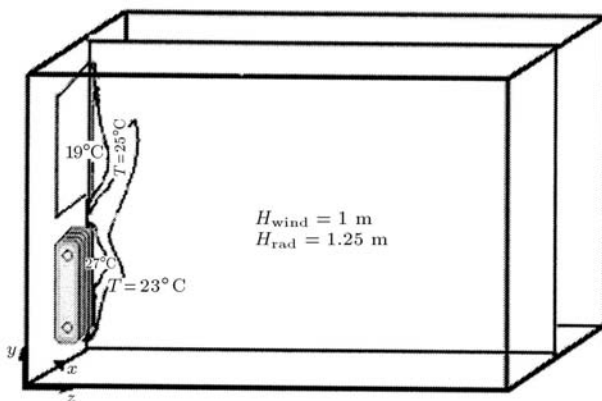


**Figure 15.** Room air temperature contours with one window and one radiator on the same wall at  $x/L = 0.5$ .

height. As shown in the figures, the strong air flow direction changes from upwards to downwards when the height of the radiator changes from 1.25 m to 0.75 m, respectively. In addition, the air temperature contours next to the respective radiators are 25°C and 20°C, respectively. Comparison of Figures 13 and 14

also show that the upward warm jet next to the larger radiator is stronger than the downward cold jet next to the window.

Figures 13 and 15 illustrate two cases in which the height of the radiators are different in each room but with the same window height. There is a strong air flow, the direction of which changes from upwards to downwards when the height of the radiator changes from 1.25 m to 0.75 m, respectively. In addition, the air temperature contours next to the respective radiators are 25°C and 20°C, respectively. A comparison of Figures 13 and 15 also shows that the upward warm jet next to the larger radiator is stronger than the downward cold jet next to the window.

Finally, Figure 14 illustrates the heat flux from the radiator and to the window versus the room temperature. It is clear that the two lines have the same trend, because, in the steady state case, the heat loss from the radiator should be identical to the heat gain by the window. The results indicate that increasing the room temperature causes the heat loss increases from the window. On the other hand, a one degree centigrade increment of the room temperature results in a 6% increase in the heat gain by the window.

## CONCLUSION

This paper proposes a two-layer, zero equation, turbulent model for prediction of the room air flow pattern and temperature. The model is derived from Navier-Stokes equations, using the concept of eddy-viscosity. The main difference between this model and the conventional CFD approach, with the  $k - \epsilon$  model, is that the former does not need to solve the transport equations for the turbulent quantities. The results demonstrate the capability of the two-layer zero equation model by applying it to stagnant air with buoyancy affected flow in a room, such as natural convection. This model can predict reasonably good indoor airflow pattern and air temperature distribution. Since the two-layer zero equation model does not solve the transport equations for turbulence, the computer memory needed for calculations is much smaller and the convergence speed is 10 times faster than that of the  $k - \epsilon$  model.

The best temperature distribution and comfort conditions are obtained when the radiator is installed under the window and its height is equal to, or greater than, that of the window. The distance between the radiator and the window does not have a major effect on the temperature distribution in the room, but increasing the distance between the window and the radiator results in decreasing heat loss from the window.

**NOMENCLATURE**

$b$	constant
$C_P$	specific heat
$D$	diffusivity, $\nu/\Delta x$ or $\alpha/\Delta x$
$F$	flux, $\rho u$ , $\rho v$ , or $\rho w$
$g$	gravity acceleration
$H$	height
$I$	turbulence intensity
$k$	thermal conductivity
$K$	turbulence kinetic energy
$l$	characteristic length
$L$	length
$P$	pressure
$p_{\text{return}}$	pressure at return
$Ra$	Rayleigh number $g\beta(T_h - T_c)\overline{H}^3/\alpha\nu$
$S$	source term
$T$	temperature
$u$	$x$ -component velocity
$v$	$y$ -component velocity
$V$	velocity vector
$w$	$z$ -component velocity
$W$	width
$x$	$x$ -coordinate
$y$	$y$ -coordinate
$z$	$z$ -coordinate

**Greek Letters**

$\alpha$	thermal diffusivity
$\beta$	expansion coefficient
$\mu$	viscosity
$\rho$	density
$\phi$	fluid property
$\nu$	kinetic viscosity

**Subscript**

$c$	cold
$h$	hot
in	inlet
$m$	mixing
out	outlet
ref	reference

$t$             turbulent

**Superscript**

+	dimensionless
–	average

**REFERENCES**

- Olsen, D.A., Glicksman, L.R. and Ferm, H.M. "Steady state natural convection in a empty and partitioned enclosure at high Rayleigh numbers", *J. Heat Transfer, Trans. ASME*, **112**, pp 640-647 (1990).
- Ball, K.S. and Bergman, T.L. "Numerical simulation of unsteady low Pr convection using a Chebyshev collection technique", *ASME Paper*, 93-WA/HA-43 (1993)
- Peeters, T.W. and Hanks, R.A. "The Reynolds-stress model of turbulence applied to the natural-convection boundary layer along a heated vertical plate", *Int. J. Heat Mass Transfer*, **35**, pp 403-420 (1992).
- Cheesewright, R. "Turbulent natural convection from a vertical plane surface", *Transaction of ASME, Journal of Heat Transfer*, pp 1-9 (1968).
- Chen, Q., Hoornsta, T.G. and van der Kooi, J. "Energy analysis of building with different air supply and exhaust system", *ASHREA Transaction*, **96**(1), pp 344-356 (1990).
- Schwenke, H. "Ueber das verhalten elener horizontaler zuluftstrahlem im begrenzten raum", *Luft und Kaltetchnik*, **5**, pp 241-246 (1975).
- Blay, D., Mergui, S. and Niculae, C. "Confined turbulent mixed convection in presence of a horizontal buoyant wall jet", *Fundamental of Mixed Convection*, HTD213:65-72 (1992).
- Prandtl, L. "Uber die asugebildete turbulenze", *ZAMM*, **5**, pp 136-139 (1925).
- Van Driest, E.R. "On turbulent flow near a wall", *Journal of the Aeronautical Science*, **23**, p 1007 (1956).
- Chen, Q. and Xu, W. "New turbulence model for indoor air flow simulation", Massachusetts Institute of Technology, Ph.D Thesis (1998).
- Versteeg, H.K. and Malalasekera, W. *An Introduction to Computational Fluid Dynamics*, John Wiley & Sons Inc., New York (1995).
- Patankar, S.V. *Numerical Heat Transfer and Fluid Flow*, New York, Hemisphere (1980).